

# Vibrational emission analysis of the CN molecules in laser-induced breakdown spectroscopy of organic compounds

Ángel Fernández-Bravo, Tomás Delgado, Patricia Lucena, J. Javier Laserna \*

Department of Analytical Chemistry, University of Málaga, E-29071 Málaga, Spain

Corresponding author. E-mail address: laserna@uma.es (J.J. Laserna)

## Abstract

Laser-induced breakdown spectroscopy (LIBS) of organic materials is based on the analysis of atomic and ionic emission lines and on a few molecular bands, the most important being the CN violet system and the C<sub>2</sub> Swan system. This paper is focused in molecular emission of LIBS plasmas based on the CN ( $B^2\Sigma-X^2\Sigma$ ) band, one of the strongest emissions appearing in all carbon materials when analyzed in air atmosphere. An analysis of this band with sufficient spectral resolution provides a great deal of information on the molecule, which has revealed that valuable information can be obtained from the plume chemistry and dynamics affecting the excitation mechanisms of the molecules. The vibrational emission of this molecular band has been investigated to establish the dependence of this emission on the molecular structure of the materials. The paper shows that excitation/ emission phenomena of molecular species observed in the plume depend strongly on the time interval selected and on the irradiance deposited on the sample surface. Precise time resolved LIBS measurements are needed for the observation of distinctive CN emission. For the organic compounds studied, larger differences in the behavior of the vibrational emission occur at early stages after plasma ignition. Since molecular emission is generally more complex than that involving atomic emission, local plasma conditions as well as plume chemistry may induce changes in vibrational emission of molecules. As a consequence, alterations in the distribution of the emissions occur in terms of relative intensities, being sensitive to the molecular structure of every single material.

**Keywords:** LIBS, Molecular bands, Vibrational emission analysis, Polymer identification

## Introduction

Removal of material from a sample surface can be accomplished by use of laser irradiation, and this process is called laser ablation [1–5]. Ablation primarily produces ionization of the samples and optical emission of the species at a sufficient level of irradiance. Laser-induced breakdown spectroscopy (LIBS) allows us to spectrally analyze the laser ablation plasma [6,7]. The plasma formed in the ablation contains information on the constituents of the samples. The information presented in a LIBS spectrum is, in most of the cases, elemental information, being extensively used for discriminating between materials with a different elemental composition [8,9]. The applications of LIBS show remarkable versatility and include, for example, industry, archeological studies, chemical imaging of historical buildings and Chemcam investigations among others [10–13]. LIBS can also be combined with other laser-based techniques such as Raman spectroscopy, enhancing the capabilities of LIBS for organic compound discrimination [14]. However, some drawbacks are presented in LIBS when attempts are made to analyze organic materials with similar elemental composition. In the last two decades, organic compound analysis using LIBS has involved the use of other spectroscopic information recorded in organic spectra such as molecular bands [15–17]. There are few molecular bands in an open air LIBS spectrum, namely CN and C<sub>2</sub> [18]. The molecular information is usually similar in all organic compounds, and discrimination based on the emissions of the fundamental transition is not always possible. However, an exhaustive exploration of the molecular spectrum with adequate resolution offers a great deal of information that deserves to be explored [19]. Future improvements of LIBS as a tool for organic material analysis may require an appropriate molecular spectral interpretation.

In most cases, atomic emission is associated with a single transition producing a line at a discrete wavelength, whereas emission of molecules is associated with a group of emission lines corresponding to vibrational states, which are derived from electronic transitions of the molecules and are known as vibrational emissions. Although molecular emission has been widely studied [20–23], vibrational emission of molecules is not so often investigated in LIBS [24–27]. The response of CN molecule emission to laser ablation has a great potential since CN is presented in every carbon material when ablated in the presence of nitrogen. Furthermore, the signal-to-noise ratio of this molecular band is usually the highest in organic LIBS spectra. This emission and its relation to the molecular structure can disclose useful information for the distinction of organics by LIBS and a deeper understanding of the principal formation routes of CN and other species existing in laser-induced plasmas. The knowledge of the mechanisms involved in molecular excitation and reactivity in the plume will help to increase the quality of the analysis [23,28–30].

The complexity of the ablation products may vary from one material to another, altering the chemistry of the plume. There are two major pathways for CN formation, namely, by direct fragmentation of the materials with structural carbon–nitrogen bonds, called native CN, or by secondary processes such as atomic reactive recombination, which is always present in more or less proportion. This fact is one of the main differentiating mediators in CN emission. The native CN is appearing in the spectra at early times after plasma formation, whereas CN formed by reactive recombination presents a delay in its emission [31]. The reactive atomic recombination needs nitrogen from the surroundings to form CN and the location of the molecules in the plasma can be different from that of the molecules that follow other reaction pathways. In this sense molecules are sensitive to local conditions of the plasma.

This paper offers a fresh perspective on the use of the molecular information from LIBS spectra of organic materials, based on the study of the vibrational emission of the CN molecular bands. Molecular emission in laser-induced plasmas is demonstrated to depend on experimental conditions such as the time evolution and the laser pulse irradiance. The variation with time of the vibrational distribution of the molecules plays a key role in the observed emissions. Also, the vibrational transitions exhibit different sensitivities to a variation

of the laser pulse irradiance. These two factors are thus markedly important when studying the LIBS spectra of organic molecules. The intensity distribution of vibrational transitions has been investigated for different polymers. A relation between vibrational emission of CN and molecular structure of the analyzed materials is suggested. A detailed investigation of vibrational LIBS emission of CN molecules in polymers has revealed that additional information can be obtained from organic materials from the mere measurement of integrated band intensities.

### 1.1. Experimental set-up

A pulsed Nd:YAG laser (Ekspla, model NL 303D/SH; @ 1064 nm, 10 Hz, pulse width 4 ns) was used for LIBS experiments. The experiments were carried out at room temperature and without any control of either pressure or atmosphere. The laser beam was guided and focused onto the surface of the material through a system of mirrors and a plano-convex lens with a focal length of 175 mm. Plasma light was collected through a fiber optic onto the entrance slit of an echelle spectrometer (ME-5000 i-Star, DH734, 190 mm, F/7), with an attached intensified CCD detector (1024 × 1024 pixels). The grating has 52.13 grooves/mm, the slit-width is 50 μm and the camera pixel size is 13 μm, the spectral resolution is FWHM of 0.097 nm at 388 nm (4 pixels FWHM). The spectral range comes from 200 to 950 nm. The wavelength calibration was carried out using a Hg lamp. The sensitivity correction was accomplished with a certificated reference deuterium/halogen lamp.

Spectroscopic imaging experiment was carried out by filtering plasma light by two narrowband filters, 10 nm width centered at 385 nm for CN emission and 40 nm width centered at 760 nm for N + O emission. The filtered plasma light was focused through a 100 mm focal length lens with magnification ×1 into an i-CCD detector, used in imaging mode.

### 1.2. Samples

Five organic polymers were used in this work: nylon, Teflon, polystyrene (PS), polypropylene (PP) and polyvinyl chloride (PVC). Materials are listed in Table 1, showing the molecular formula and the monomeric structure of the polymers.

## 2. Results and discussion

LIBS has been used for the analysis of organic compounds with very promising results in terms of qualitative analysis, but still one of the most difficult tasks involves the discrimination power and identity assignment between them. In general, all organics present very similar emission features, either molecular bands or atomic lines (CN, C<sub>2</sub>, C(I), H(I), N(I) and O(I)) and only subtle differences are observed between them. Molecular emissions become important as they are the major source of information available in the spectra [31–33].

Fig. 1(A) shows time integrated LIBS spectra of nylon, polystyrene and Teflon in the CN emission spectral region. As shown, only subtle differences in the intensity of CN band at 388.2 nm ( $\Delta v = 0$  sequence) can be observed, polystyrene showing the strongest emission. However, a group of emissions corresponding to transitions between electronic states of CN, known as vibrational emission, are also observed. Fig. 1(B) shows a schematic diagram of the transitions involved. The most probable emission is associated with those levels that present less energy requirements, i.e., transitions between the lowest vibrational states [19]. The relative intensities of the lowest vibrational states are considerably stronger than those associated with the highest vibrational states.

Interestingly, however, a detailed analysis of the band structure reveals significant differences between the emissions of these compounds. In order to see these differences a careful study of the measurement timing must be done.

Fig. 2 presents spectra of Teflon at different timing conditions. As shown, the vibrational emission of the CN band changes at shorter delay times with respect to the spectrum observed at longer delays. In this case, no significant differences with respect to time-integrated spectra are observed (see Fig. 1). Among other reasons, this behavior is due to the well known larger temperature and electron number density existing in the plasma at early times. The effect of plasma parameters on the emission of the CN system is in this sense similar to the dependence of intensities of atomic and ionic lines: a larger plasma temperature should result in the increased population of high energy levels, namely, the 4-4 transitions, as compared to the lower levels, or the 0-0 transition.

In a similar fashion, the peak height distribution should depend on the energy deposited at the target. Fig. 3 shows spectra of Teflon at two irradiances. At  $31.2 \text{ GW cm}^{-2}$ , the spectrum follows the equilibrium distribution of intensities, with the 0-0 transition as the most intense line of the  $\Delta v = 0$  sequence. At the larger irradiance of  $62.5 \text{ GW cm}^{-2}$ , the most intense peak corresponds to the 3-3 vibrational transition (385.59 nm). The different polymers tested respond to a different extent to the timing parameters and the fluence. The rationale for these results will be discussed below.

Time-resolved spectroscopic imaging with narrowband filters was used for the simultaneous monitoring of the spatial and temporal distribution of species in the plume [34,35]. Fig. 4 shows time-resolved spectroscopic images of plasmas generated in Teflon and nylon. The CN emission was acquired across the plasma plume through a 10-nm narrowband filter centered at 385 nm. The emissions of N and O were filtered by a 40 nm band width centered at 760 nm.

At early stages from plasma ignition (100 ns) the CN emission is observed as a bright spot close to the sample surface. Later, the CN detaches from the surface as it is clearly seen from 600 ns onwards. As structural nitrogen and native CN bonds are present only in nylon, the emission at very short delay times show the nascent band in nylon with a high contribution of structural nitrogen. In Teflon the CN is due to reaction of C dissociated from the original molecule with atmospheric nitrogen, probably by air entrainment in the plasma. Thus, the different behavior of the CN emissions observed is due to the different origin of the molecule. On the other hand, after a delay of ca. 500 ns, the integrated CN emissions in Teflon are preferentially located at the top part of the plume, whereas in nylon, the largest abundance of CN is situated close to the sample surface.

As commented above, some of the CN emissions observed must derive from reactions of carbon with atmospheric nitrogen. In this sense, space segregation of different species such as nitrogen and oxygen inside of the plasma will critically influence CN emission. Structural nitrogen in nylon produces a bright core of nitrogen emission close to the sample surface, whereas the Teflon plasma exhibits an elongation of the plume in the direction of the incoming laser beam. This is probably one of the responsible factors of the location of CN species in the top side of Teflon plasma, since the nitrogen population is increased in this part compared with nylon.

## 2.1. Time-resolved analysis of the CN vibrational emission

Local conditions in the plasma may induce distinctive spectroscopic features in the CN molecular band, which can modify the emission itself in the sense of altering the vibrational emission distribution. Time-resolved analysis of the vibrational emissions is a good option to monitor the influence of the local conditions over the molecular emission of CN [36].

Fig. 5 shows the net intensity of two transitions of CN as well as one transition of C<sub>2</sub> fundamental mode emission versus time for nylon and Teflon. As shown in Fig. 5(A), the emission of the particular vibrational transition (0-0) at 388.26 nm of CN for both materials presents a similar trend, being slightly different at short delay times. The main limitation in using CN band for identification of organics by LIBS derives from the use of the emission band head of the CN for such a purpose [18,32]. As mentioned before, the (0-0) band of CN has lower energetic requirements and larger relative intensities than the other transitions, hence it has a lower dependence on the material composition. So, very few variations are expected between materials for this fundamental transition. However, Fig. 5(B) shows that the

emission of the (4-4) vibrational transition at 385.09 nm presents different intensities in each material at delays shorter than 700 ns. The trend presented by this mode is different than the exhibited by the fundamental emission. Thus, the use of other transitions from the vibrational structure of the band may have several advantages. One of the most relevant and pursued issue in this paper is to establish a relation between the emission of the CN vibrational transitions and material composition.

## 2.2. Effect of irradiance in vibrational emission

Fig. 6 shows the net intensity of CN at 388.25 nm (0-0), 385.39 nm (3-3) and 385.09 nm (4-4) as a function of irradiance for nylon, polystyrene and Teflon. The intensity of relevant atomic emission lines is also plotted.

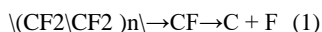
The intensities of the vibrational transitions have grown along with the irradiance after the onset of the molecular emission. For nylon Fig. 6(A) indicates that the maximum intensity is observed at 42 GW cm<sup>-2</sup> to decrease afterwards. At 62 GW cm<sup>-2</sup> the signal disappears for the three modes, most probably due to a dissociation of the CN molecules. The fundamental emission at 388.25 nm is the most prominent in the whole range of irradiance studied.

As Fig. 6(B) shows, polystyrene emissions present a similar trend to nylon, but in this case the three emissions plotted show a parallel sensitivity to the increased irradiance. If different plume chemistry between nylon and polystyrene is assumed because of the structural differences among the compounds (presence of aromatic ring in polystyrene and structural nitrogen in nylon), the generation routes followed by CN in each material could be also be different. On the other hand, differential energetic requirements for the formation of CN in the plume of each material allows those transitions in polystyrene (3-3; 4-4), while they are not favored in nylon.

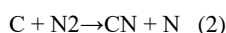
Fig. 6(C) shows the CN band emission of Teflon, where a relative maximum for the three transitions represented is observed at 42 GW cm<sup>-2</sup>. However, the emissions continue to grow from 50 GW cm<sup>-2</sup> to 70 GW cm<sup>-2</sup>. This different behavior as compared to nylon and polystyrene suggests that competitive routes for the generation of CN may coexist and alternative excitation pathways are modifying the vibrational emission.

Fig. 6(D)–(F) shows the atomic emission of N (I), O (I) and H (I) for the three polymers presented in this section. The atomic emission intensity increased proportionally with the increased irradiance. Comparing the atomic emissions with molecular bands in nylon and polystyrene, high irradiances (50 GW cm<sup>-2</sup>) produced an increase in atomic emission in detriment of molecular emission. Probably, a high input energy in the plume prevents the formation of stable molecules. Atomic emissions in Teflon kept growing in the whole irradiance range.

Fig. 6(G) and (H) shows the net intensity of the atomic line of C at 247.85 nm for the polymers investigated. A similar trend with the other atomic lines is observed. The atomic line of F at 685.56 nm is shown in Fig. 6(I). The intensity also increases with the irradiance as with other atomic lines. However, the F line exhibits a sudden increase in intensity at 65 GW cm<sup>-2</sup>, which coincides with the increase in CN intensity observed in the high irradiance regime (Fig. 6(C)). In this case, it is suggested that the increased intensity of F and CN is due to the dissociation at high irradiance of the CF molecule released from the polymer, according to the following reaction:



where the new source of atomic carbon (reaction (1)) favors the formation of CN in a subsequent reaction [37],



and the abundance of F grows through reaction (1). This fact is captured in Fig. 6(I) as the increased emission of F at irradiance beyond 65 GW cm<sup>-2</sup>. This mechanism would be also responsible for the observed behavior that the CN intensity in Teflon continues growing with increasing the laser irradiance as observed in Fig. 6(C). Differently, all other polymers tested exhibit the opposite behavior, i.e., the intensity of CN decreases with the irradiance beyond 45 GW cm<sup>-2</sup> (see Fig. 6(A) and (B) for the case of nylon and polystyrene).

### 2.3. Vibrational emission dependence on molecular structure

For the five polymers studied, Fig. 7 shows CN normalized intensities of the five spectral transitions at an irradiance of  $44 \text{ GW cm}^{-2}$ , using a delay time of 500 ns and integrated for 500 ns. As the figure reveals, two groups of compounds can be distinguished according to their vibrational structure. In polymers containing halogens (PVC and Teflon), the vibrational distribution of the CN band is distorted in such a way that the 4-4 vibrational transition is more intense than the lower energy transitions 1-1, 2-2, 3-3. In the absence of halogens (PS, nylon, and PP), the polymers exhibit the regular intensity distribution. This distorted behavior is due to the vibrational excitation of the CN fragment/molecule, since the molecule is formed in a highly energetic plasma, where the main excitation process should be electron impact and the de-excitation process the collisional quenching [37–39].

### 3. Conclusions

In this paper, an investigation of CN emission in laser-induced plasmas of polymers reveals that additional information can be obtained from the vibrational structure of this band to that obtained from the mere measurement of integrated band intensities. Precise time resolved LIBS measurements are needed for observation of distinctive CN vibrational emission. For the organic compounds studied, larger differences in the behavior of the transition emission occur at early stages after plasma formation. Most energetic transitions of the vibrational structure are notably more sensitive to time evolution than those with less energetic requirements.

The laser pulse irradiance influences dramatically the LIBS spectra of organic compounds, affecting both the intensity of the atomic and molecular emissions and the vibrational emission of CN molecules. In general, high irradiance values favor atomic emissions, but an upper irradiance level not always involves an enhanced intensity of molecular bands, as demonstrated for nylon and polystyrene. In Teflon, a different trend in molecular emission with the irradiance is observed. At high irradiance values, dissociation of fragments/molecules such as CF plays a distinctive role in the sense of becoming a new carbon source for CN formation, but also modifying the chemistry of the plasma. The material signature is diluted with time due to recombination and diffusion processes of the species into the plume and with the atmosphere surrounding the plasma.

### Acknowledgments

Research supported by the Excellence Project P07-FQM-03308 of the Secretaría General de Universidades, Investigación y Tecnología, Consejería de Innovación, Ciencia y Empresa de la Junta de Andalucía.

### References

- [1] L.J. Radziemski, Review of selected analytical applications of laser plasmas and laser ablation, 1987–1994, *Microchem. J.* 50 (1994) 218–234.
- [2] A. Vertes, *Laser Ablation: Mechanisms and Applications II*, Chapter Energy Coupling and Dissipation Mechanisms in Laser–Solid Interaction, AIP Press, Knoxville, 1994. 275–284.
- [3] R. Haglund, Microscopic and mesoscopic aspects of laser-induced desorption and ablation, *Appl. Surf. Sci.* 96–98 (1996) 1–13.
- [4] C. Phipps, *Laser Ablation and its Applications*, Springer, New York, 2007.
- [5] A. Fernández-Bravo, P. Lucena, J.J. Laserna, Selective sampling and laser-induced breakdown spectroscopy (LIBS) analysis of organic explosive residues on polymer surfaces, *Appl. Spectrosc.* 66 (2012) 1197–1203.
- [6] D.A. Cremers, A.K. Knight, Laser-induced breakdown spectroscopy, *Encyclopedia of Analytical Chemistry*,

vol. 11, Wiley, New York, 2000.

- [7] D.A. Cremers, L.J. Radziemski, *Handbook of Laser-Induced Breakdown Spectroscopy*, John Wiley & Sons, Ltd., Chichester, 2006.
- [8] J. Cuñat, F.J. Fortes, L.M. Cabalín, F. Carrasco, M.D. Simón, J.J. Laserna, Man-portable laser-induced breakdown spectroscopy system for in situ characterization of karstic formations, *Appl. Spectrosc.* 62 (2008) 1250–1255.
- [9] F.J. Fortes, L.M. Cabalín, J.J. Laserna, The potential of laser-induced breakdown spectrometry for real time monitoring the laser cleaning of archaeometallurgical objects, *Spectrochim. Acta Part B* 63 (2008) 1191–1197.
- [10] R. Noll, H. Bette, A. Brysch, M. Kraushaar, I. Monch, L. Peter, V. Sturm, Laser-induced breakdown spectrometry applications for production control and quality assurance in the steel industry, *Spectrochim. Acta Part B* 56 (2001) 637–649.
- [11] F.J. Fortes, M. Cortés, M.D. Simón, L.M. Cabalín, J.J. Laserna, Chronocultural sorting of archaeological bronze objects using laser-induced breakdown spectrometry, *Anal. Chim. Acta* 554 (2005) 136–143.
- [12] F.J. Fortes, J. Cuñat, L.M. Cabalín, J.J. Laserna, In-situ analytical assessment and chemical imaging of historical buildings using a man-portable laser system, *Appl. Spectrosc.* 61 (2007) 558–564.
- [13] P. Sobron, A. Wang, F. Sobron, Extraction of compositional and hydration information of sulfates from laser-induced plasma spectra recorded under Mars atmospheric conditions — implications for Chemcam investigations on Curiosity rover, *Spectrochim. Acta Part B* 68 (2012) 1–16.
- [14] J. Moros, J.A. Lorenzo, P. Lucena, L.M. Tobaría, J.J. Laserna, Simultaneous Raman spectroscopy–laser-induced breakdown spectroscopy for instant standoff analysis of explosives using a mobile integrated sensor platform, *Anal. Chem.* 82 (2010) 1389–1400.
- [15] S.S. Harilal, R.C. Issac, C.V. Bindhu, V.P.N. Nampoori, C.P.G. Vallabhan, Optical emission studies of C2 species in laser-produced plasma from carbon, *J. Phys. D: Appl. Phys* 30 (1997) 1703–1709.
- [16] A. Portnov, S. Rosenwaks, I. Bar, Emission following laser-induced breakdown spectroscopy of organic compounds in ambient air, *Appl. Opt.* 42 (2003) 2835–2842.
- [17] S. Abdelli-Messaci, T. Kerdja, A. Bendib, S. Malek, CN emission spectroscopy study of carbon plasma in nitrogen environment, *Spectrochim. Acta Part B* 60 (2005) 955–959.
- [18] F.C. De Lucia Jr., J.L. Gottfried, C.A. Munson, A.W. Miziolek, Double pulse laser-induced breakdown spectroscopy of explosives: initial study towards improved discrimination, *Spectrochim. Acta Part B* 62 (2007) 1399–1404.
- [19] W. Demtroder, *Molecular physics, Theoretical Principles and Experimental Methods*, Wiley-VCH, Weinheim, 2005.
- [20] G. Jihua, A. Ali, P.J. Dagdigian, State-to-state collisional interelectronic and intraelectronic energy transfer involving CN A2Π v = 3 and X2 Σ+ v = 7 rotational levels, *J. Chem. Phys.* 85 (1986) 7098–7105.
- [21] D.G. Sauder, D. Patel-Misra, P.J. Dagdigian, The vibronic state distribution of the NCO(X2Π) product from the CN + O2 reaction, *J. Chem. Phys.* 95 (1991) 1696–1707.
- [22] B. Nizamov, P.J. Dagdigian, M.H. Alexander, State-resolved rotationally inelastic collisions of highly rotationally excited CN (A2Π) with helium: Influence of the interaction potential, *J. Chem. Phys.* 115 (2001) 8393–8402.
- [23] P. Lucena, A. Doña, L.M. Tobaría, J.J. Laserna, New challenges and insights in the detection and spectral identification of organic explosives by laser induced breakdown spectroscopy, *Spectrochim. Acta Part B* 66 (2011) 12–20.
- [24] J.O. Hornkohl, C. Parigger, J.W.L. Lewis, Temperature measurements from CN spectra in a laser-induced

plasma, *J. Quant. Spectrosc. Radiat. Transfer* 46 (1991) 405–411.

[25] L. Nemes, A.M. Keszler, J.O. Hornkohl, C.G. Parigger, Laser-induced carbon plasma emission spectroscopic measurements on solid targets and in gas-phase optical breakdown, *Appl. Optics* 44 (2005) 3661–3667.

[26] A.A. Ndiaye, V. Lago, Optical spectroscopy investigation of N<sub>2</sub>-CH<sub>4</sub> plasma jets simulating titan atmospheric entry conditions, *Plasma Sources Sci. Technol.* 20 (2011) 015015.

[27] C.G. Parigger, Atomic and molecular emissions in laser-induced breakdown spectroscopy, *Spectrochim. Acta Part B* 79–80 (2013) 4–16.

[28] P. Halvick, J.C. Rayez, M.T. Rayez, B. Duguay, Three-atom indirect exchange reactions. II. Dynamical behaviours explained by a simple model, *Chem. Phys.* 114 (1987) 375–387.

[29] N. Daugey, A. Bergeat, A. Schuck, P. Caubet, G. Dorthé, Vibrational distribution in CN(X<sup>2</sup>Σ<sup>+</sup>) from the N + C<sub>2</sub> → CN + C reaction, *Chem. Phys.* 222 (1997) 87–103.

[30] K. Sovov, K. Dryahina, P. Spane, M. Kyncl, S. Civi, A study of the composition of the products of laser-induced breakdown of hexogen, octogen, pentrite and trinitrotoluene using selected ion flow tube mass spectrometry and UV–vis spectrometry, *Analyst* 135 (2010) 1106–1114.

[31] M. Baudelet, M. Boueri, J. Yu, S.S. Mao, V. Piscitelli, X. Mao, R.E. Russo, Time-resolved ultraviolet laser-induced breakdown spectroscopy for organic material analysis, *Spectrochim. Acta Part B* 62 (2007) 1329–1334.

[32] M. Baudelet, M. Boueri, J. Yu, X. Mao, S.S. Mao, R. Russo, Laser ablation of organic materials for discrimination of bacteria in an inorganic background, *Proc. SPIE* 7214 (2009) 72140(J1-10).

[33] D.S. Moore, Recent advances in trace explosives detection instrumentation, *Sens. Imaging* 8 (2007) 9–38.

[34] V. Motto-Ros, Q.L. Ma, S. Grégoire, W.Q. Lei, X.C. Wang, F. Pelascini, F. Surma, V. Detalle, J. Yu, Dual-wavelength differential spectroscopic imaging for diagnostics of laser-induced plasma, *Spectrochim. Acta Part B* 74 (2011) 11–17.

[35] S. Grégoire, V. Motto-Ros, Q.L. Ma, W.Q. Lei, X.C. Wang, F. Pelascini, F. Surma, V. Detalle, J. Yu, Correlation between native bonds in a polymeric material and molecular emissions from the laser-induced plasma observed with space and time resolved imaging, *Spectrochim. Acta Part B* 74 (2011) 31–37.

[36] B. Nemet, K. Musiol, I. Santa, J. Zachorowski, Time-resolved vibrational and rotational emission analysis of laser-produced plasma of carbon and polymers, *J. Mol. Struct.* 511–512 (1999) 259–270.

[37] Q. Ma, P.J. Dagdigan, Kinetic model of atomic and molecular emissions in laser-induced breakdown spectroscopy of organic compounds, *Anal. Bioanal. Chem.* 400 (2011) 3193–3205.

[38] C.K. Luk, R. Bersohn, Time dependence of the fluorescence of the B state of CN, *J. Chem. Phys.* 58 (1973) 2153–2163.

[39] Y. Guotao, Y. Hongding, J. Junliu, Z. Shengli, X.R. Huang, C. Chungsun, Theoretical study on reaction mechanism of the CF radical with nitrogen dioxide, *J. Comput. Chem.* 22 (2001) 1907–1919.

Table 1  
Molecular formula and structural features of polymers investigated.

Material	Molecular formula	Structure
Polystyrene	$(C_8H_8)_n$	$\left[ \text{CH}_2 - \underset{\text{C}_6\text{H}_5}{\text{CH}} \right]_n$
Nylon	$(C_{12}H_{22}O_2N_2)_n$	$\left[ \text{HN} - (\text{CH}_2)_6 \text{HN} - \overset{\text{O}}{\parallel} \text{C} - (\text{CH}_2)_4 \overset{\text{O}}{\parallel} \text{C} \right]_n$
Polypropylene	$(C_3H_6)_n$	$\left[ \text{CH} - \text{CH}_2 \right]_n$   CH <sub>3</sub>
Polyvinyl chloride	$(C_2H_3Cl)_n$	$\left[ \text{CH}_2 - \underset{\text{Cl}}{\text{CH}} \right]_n$
Teflon	$(C_2F_4)_n$	$\left[ \text{CF}_2 - \text{CF}_2 \right]_n$

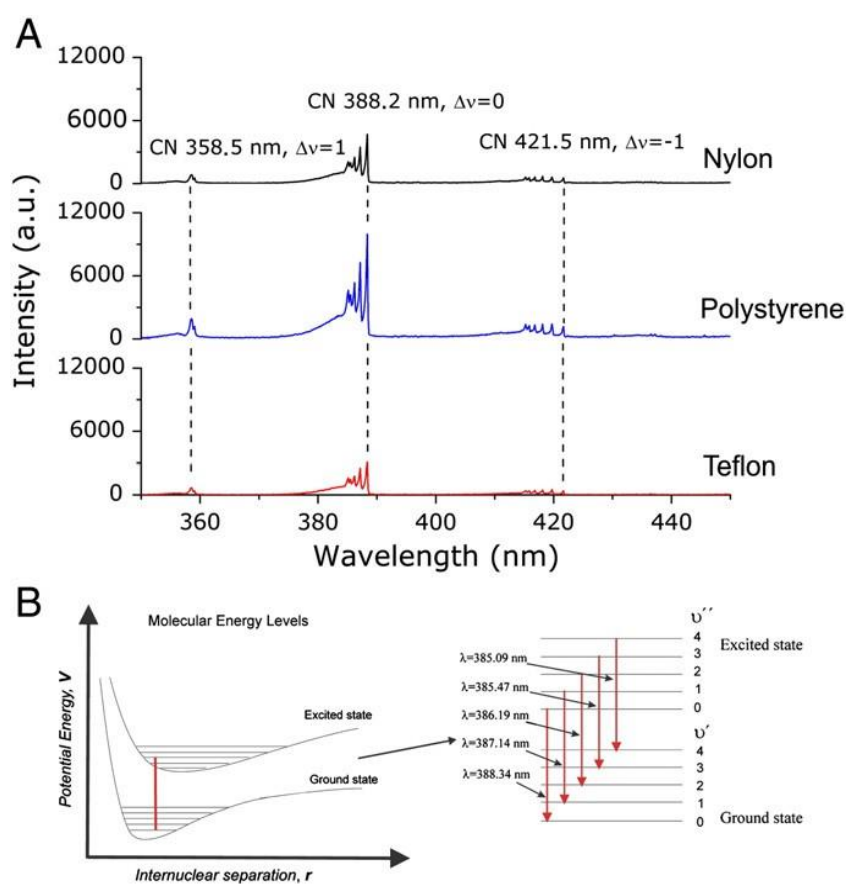


Fig. 1. (A) Time-integrated of the transitions involved in the CN vibrational emission. (B) Schematic diagram spectra of nylon, polystyrene and Teflon in the CN emission region

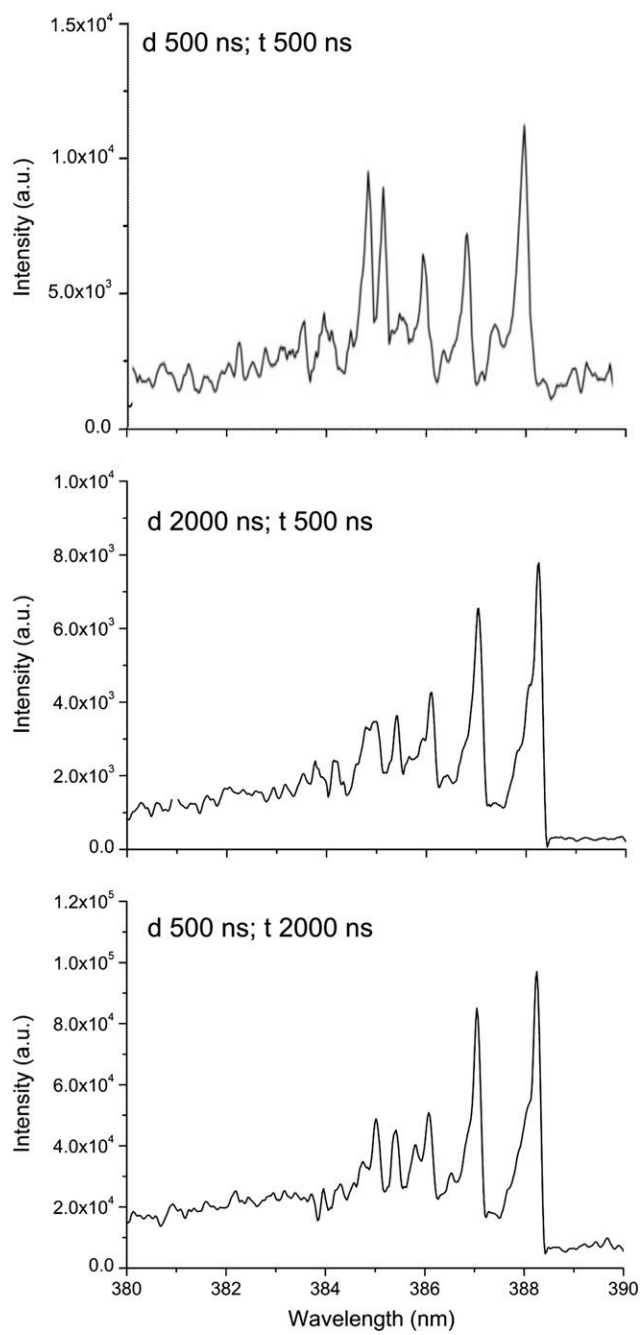


Fig. 2. Spectra of Teflon at different timing conditions.

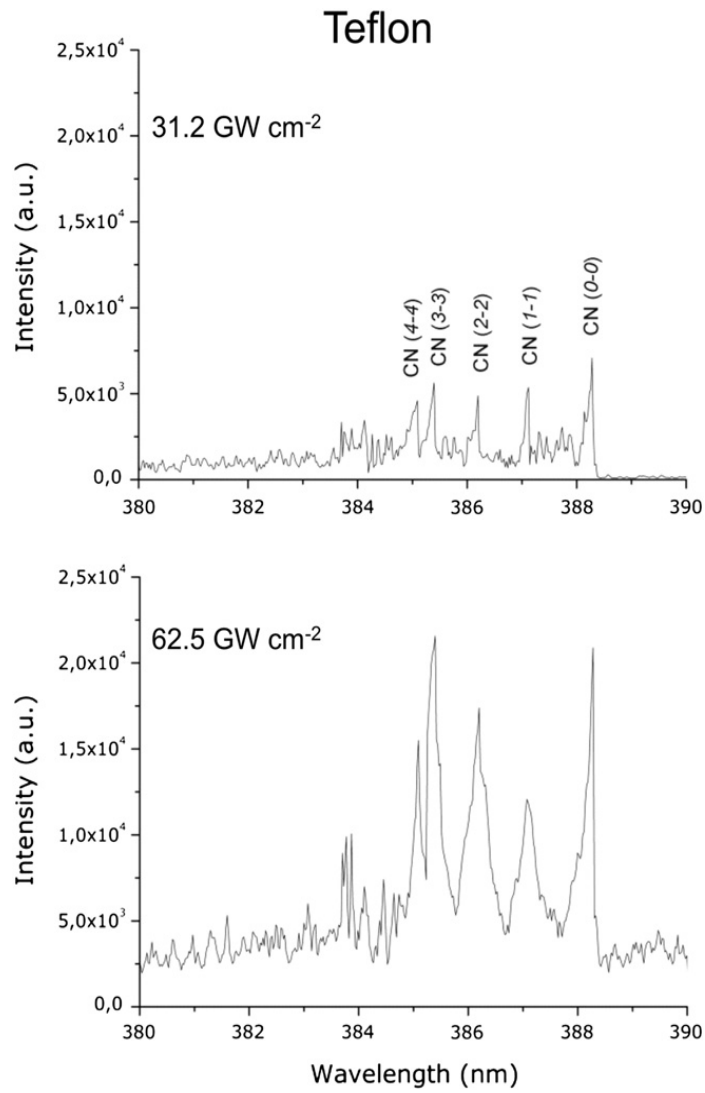


Fig. 3. Spectra Teflon in the CN molecular band emission region at two irradiances (upper panels correspond to an irradiance of 31.2 and bottom panels to 62.5 GW cm<sup>-2</sup>).

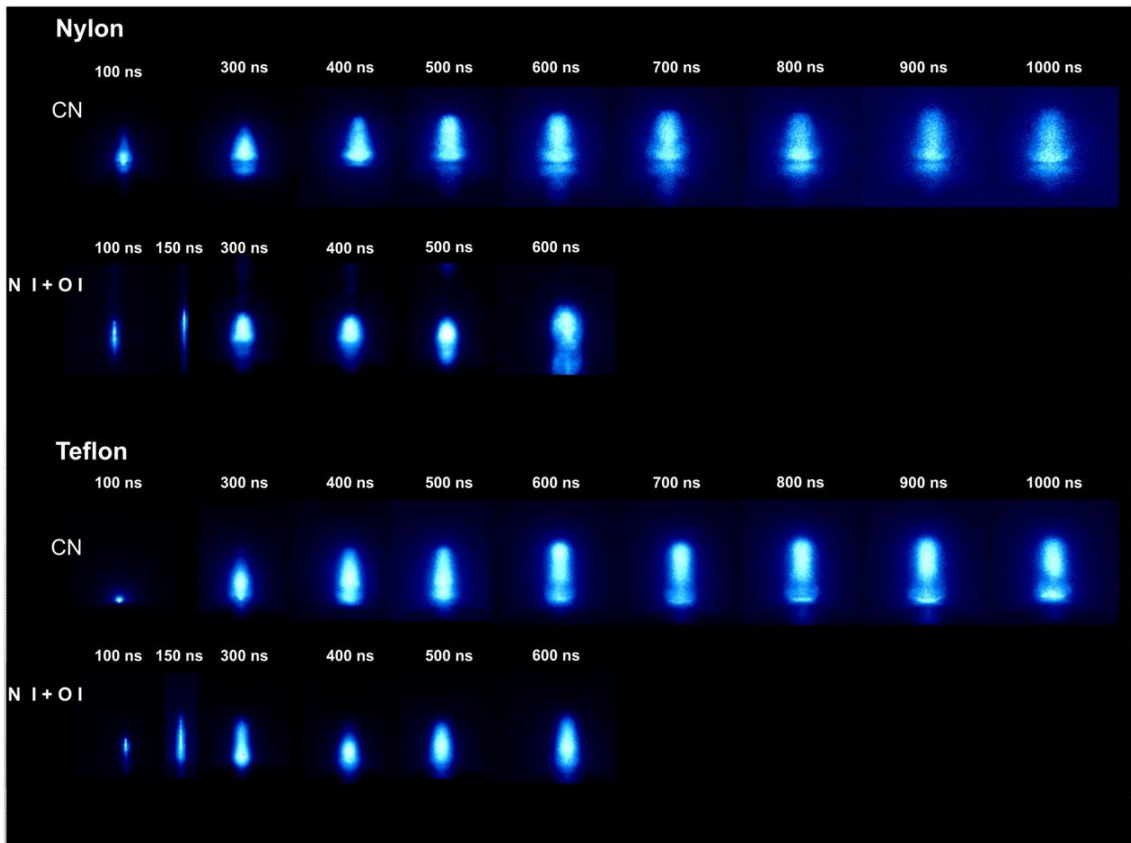


Fig. 4. Plasma i-CCD images of nylon and Teflon, showing filtered emission of CN and filtered atomic emissions of N and O.

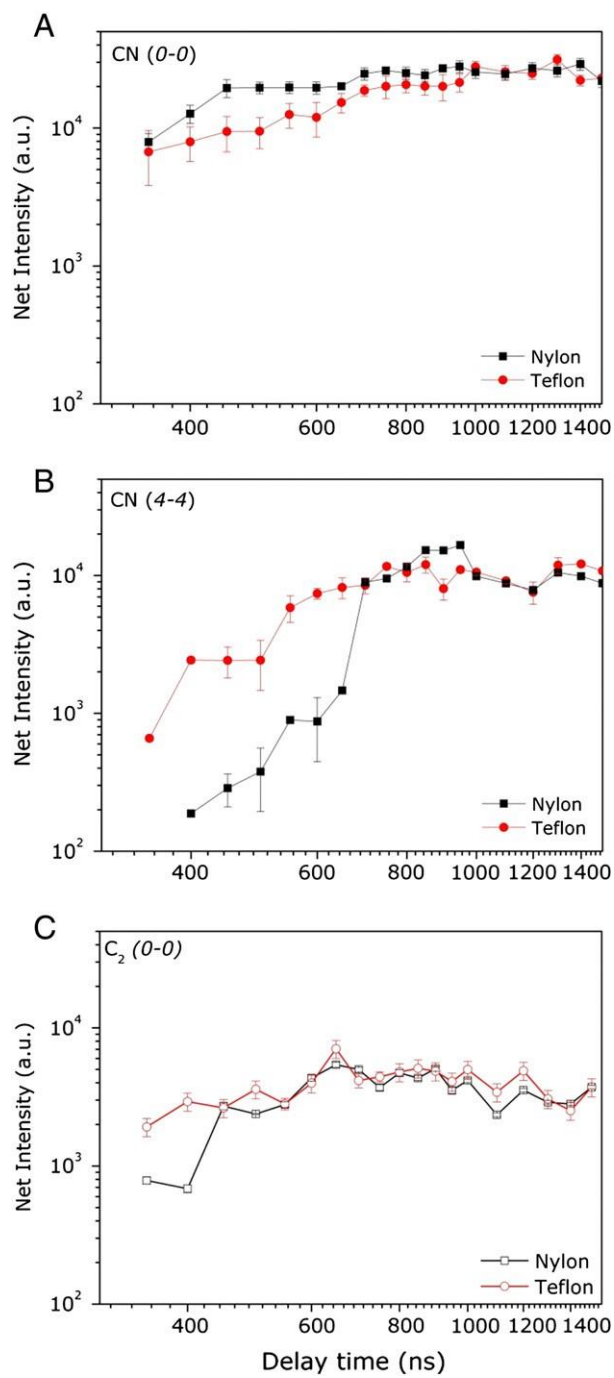


Fig. 5. Net intensity of two CN transitions as well as one transition of C<sub>2</sub> as a function of time for nylon and Teflon

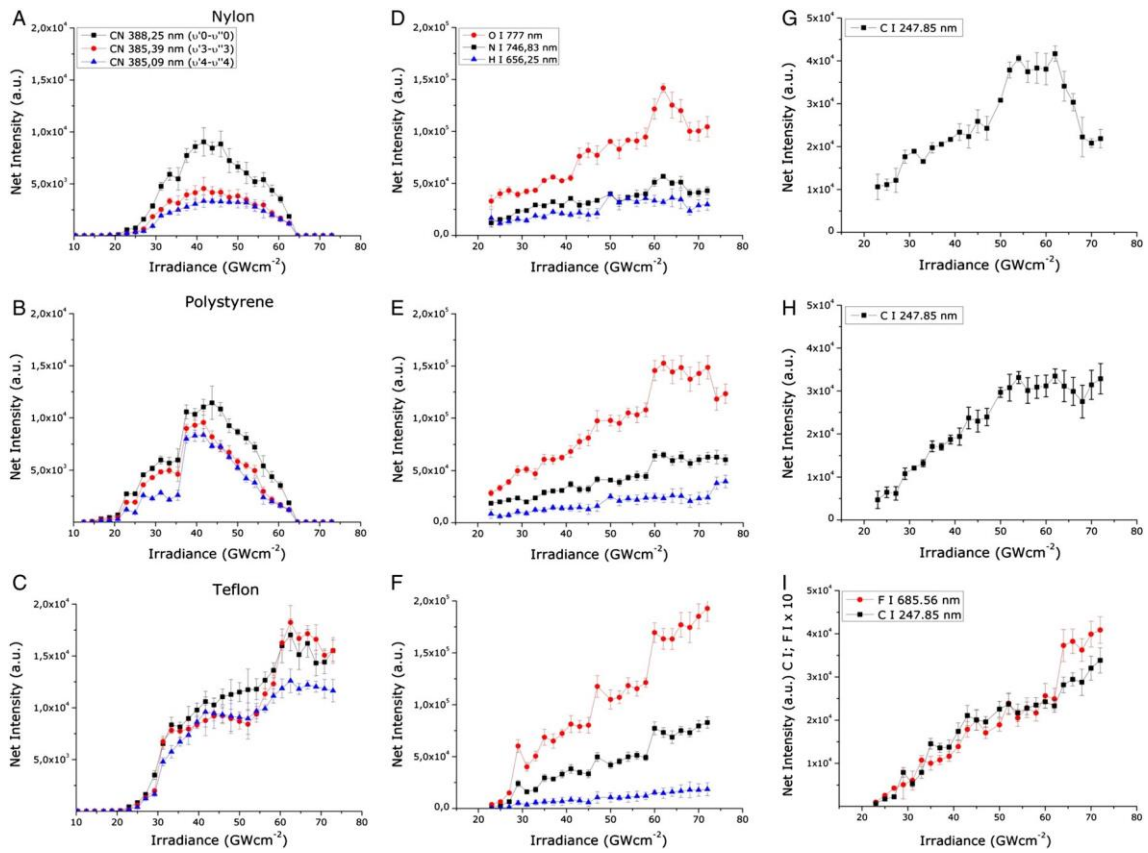


Fig. 6. Net intensity of CN molecular band at 388.25, 385.39 and 385.09 nm as a function of irradiance for (A) nylon, (B) polystyrene and (C) Teflon. Net intensity of N I 746.83 nm, O I 777 nm and H I 656.25 nm for (D) nylon, (E) polystyrene and (F) Teflon as a function of irradiance. Net intensity of atomic line C I 247.85 nm for (G) nylon (H) polystyrene and C I 247.85 nm as well as F I 685.56 nm as a function of irradiance for (I) Teflon.

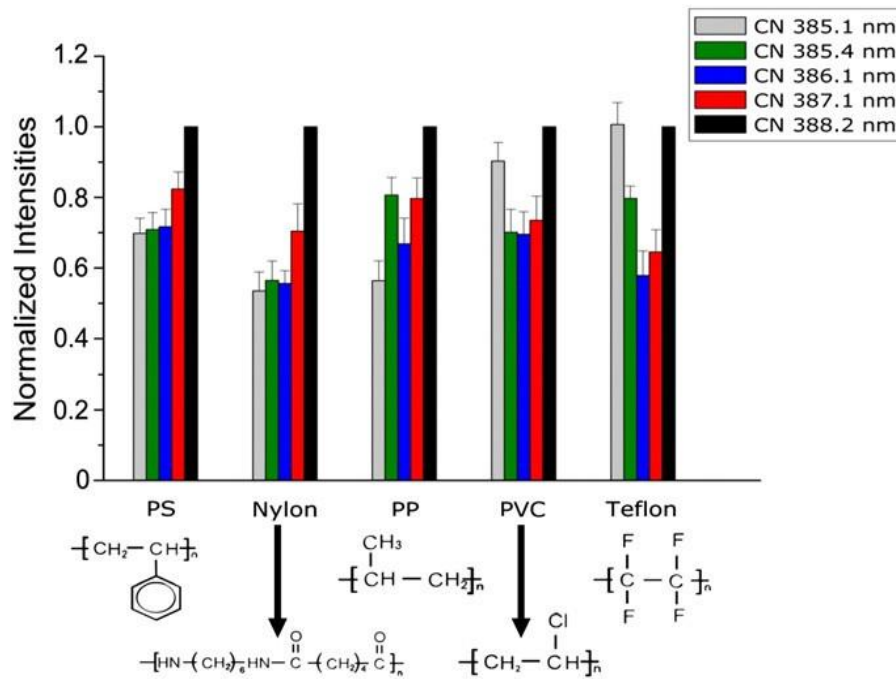


Fig. 7. Normalized intensities of CN vibrational mode five polymers at 44 GW cm<sup>-2</sup>.